Proceedings of the International Symposium on Engineering Lessons Learned from
the 2011 Great East Japan Earthquake, March 1-4, 2012, Tokyo, Japan

SITE RESPONSE CHARACTERISTICS IN SENDAI CITY ESTIMATED FROM ACCELERATION RECORDS OF THE 2011 TOHOKU EARTHQUAKE, JAPAN

Susumu OHNO[1], Masato MOTOSAKA[2], Kazuya MITSUJI[3] and Akihiro SHIBAYAMA[4]

[1] Associate Professor, Disaster Control Research Center, Tohoku University,
Sendai, Japan, ohnos@archi.tohoku.ac.jp
[2] Professor, Disaster Control Research Center, Tohoku University,
Sendai, Japan, motosaka@archi.tohoku.ac.jp
[3] Associate Professor, Faculty of Education, Art and Science, Yamagata University,
Yamagata, Japan, mitu@e.yamagata-u.ac.jp
[4] Assistant Professor, Disaster Control Research Center, Tohoku University,
Sendai, Japan, ashiba@archi.tohoku.ac.jp

ABSTRACT: Site amplifications and distribution of strong-motion spectra in Sendai, the largest city in the damaged area, are estimated for the 2011 Tohoku earthquake sequences by using the DCRC strong-motion network records and subsurface structure models in Sendai. Short-period (less than 1s) amplifications are predominant at northwestern area, while not only short but also long-period (around 3s) amplifications are predominant at southern area of Sendai.

Key Words: Great East Japan earthquake, strong motions, site amplification, Sendai

INTRODUCTION

During the M9.0 Tohoku earthquake, 3/11/2011, large accelerations were observed over the wide area along Pacific coast of Tohoku district, Japan. In the damaged area, Sendai is the largest city and had experienced the 1978 Off-Miyagi earthquake, M7.4. We have been conducting strong-motion observation in Sendai since 2004, and we obtained earthquake records during the fore, main and aftershocks of the 2011 Tohoku earthquake sequences. In this paper, we investigate the site response characteristics and estimate spatial distribution of strong-motion spectra in Sendai using this strong-motion network records.

STRONG MOTION OBSETVATION IN SENDAI

Fig.1 shows the location of observation stations in Sendai. In Sendai, there are two major strong ground motion networks: Small Titan by Tohoku Institute of Technology (Kamiyama et al., 2001; Kamiyama, 2011) and DCRC network by Disaster Control Research Center of Tohoku University (Ohno et al., 2004). Almost all DCRC stations are located on the 1st floor of low-rise building (simultaneous observation with top floor at some places).

Sendai has a complicated subsurface structure. Fig. 2 shows the depth distributions of engineering bedrock (S-wave velocity of 0.7km/s) and seismic bedrock (S-wave velocity of 3.0km/s) of subsurface structure model used for earthquake damage estimation in Sendai (Sendai City, 2002). Nagamachi-Rifu fault, a reverse-type active fault dipping to NW direction, crosses the central part of city area in NE-SW direction. West side of the fault is terrace and east side is lowland (alluvial deposits). Thickness of surface soil shallower than engineering bedrock at the ease side of the fault is up to 80m and deeper than that at the west side. On the other hand, thickness of the deep part of subsurface structure (from ground surface to seismic bedrock) becomes deeper from east to west (Watanabe and Motosaka, 2002).

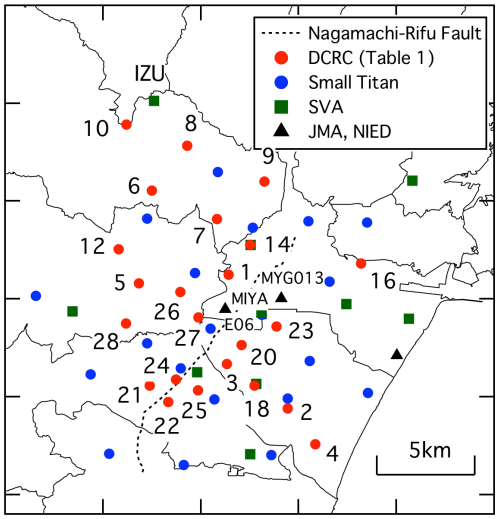

Fig. 1 Location of DCRC strong-motion stations in Sendai

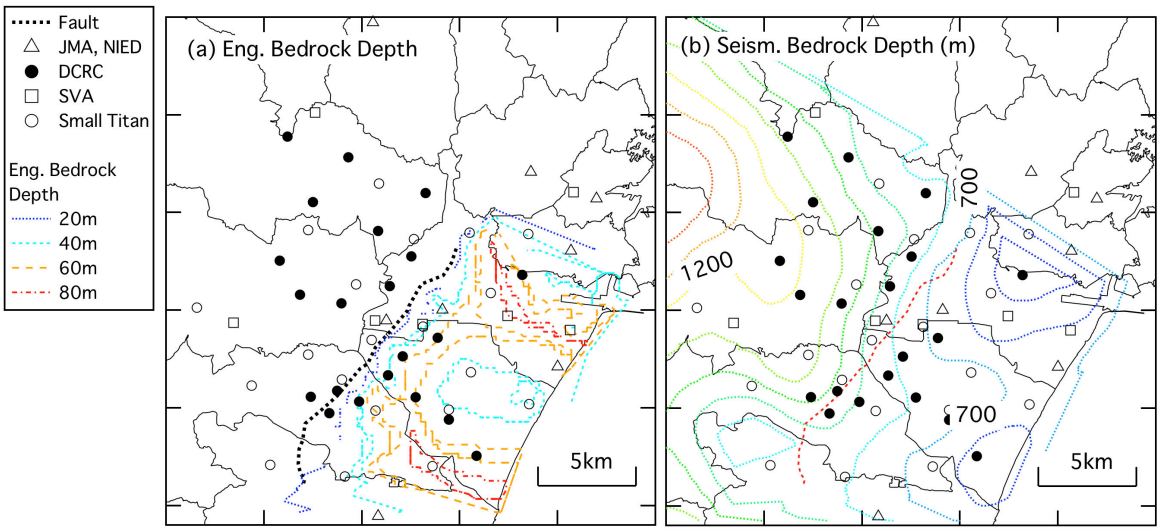

Fig. 2 Depths of engineering bedrock and seismic bedrock in Sendai (Sendai City, 2002)

Table 1 shows 1-D subsurface structure models at several DCRC stations. The models at No.8, 23, 27, and deep part (deeper than engineering bedrock) at No.25 are adopted from the 250m-mesh model of Sendai City (2002). The shallow part at No.25 is adopted from the optimized soil model for station NAGA, nearly locating at No.25, in Sendai vertical array by Satoh et al. (1994).

Table 1 1-D subsurface structure models

(a) No. 8

Width (m)	density (t/m^3)	Vs (m/s)	Soil Type
10.0	1.90	280	D
306.2	2.00	700	Pl
273.0	2.30	1300	Mi
357.9	2.40	2000	P
0	2.60	3000	

(b) No. 27

Width (m)	density (t/m^3)	Vs (m/s)	Soil Type
288.1	2.00	700	Pl
409.5	2.30	1300	Mi
227.3	2.40	2000	P
0	2.60	3000	

(c) No. 23

Width (m)	density (t/m^3)	Vs (m/s)	Soil Type
5.0	1.5	100	Ac2
15.0	2.0	450	Ag2
40.0	2.1	500	Dg
213.3	2.0	700	Pl
128.8	2.3	1300	Mi
282.1	2.4	2000	P
0	2.6	3000	

(d) No. 25

Width (m)	density (t/m^3)	Vs (m/s)	Soil Type	
0.8	1.65	105	Ac2	
4.0	1.65	105	As1	
4.5	1.95	290	Ag1	
10.9	1.70	170	Ac3	
8.2	1.75	290	Dg	
28.1	2.10	600	Dg	
24.5	1.95	530	Pl	
242.4	2.00	700	Pl	Engineering
335.4	2.30	1300	Mi	Bedrock
226.0	2.40	2000	P	
0	2.60	3000		Seismic Bedrock

D: backfill
Ac*: Holocene clay, As*: Holocene sand, Ag*: Holocene gravel;
Dg: Pleistocene Gravel
Pl: Pliocene, Mi: Miocene, P: Paleozoic

OBSERVED RECORDS

Table 2 shows a list of observation records by the DCRC network for the 3/9 foreshock, 3/11 mainshock, 4/7 and 4/11 aftershocks. During the 3/11 mainshock, records at 14 of 21 stations were obtained. PGA and PGV range 318-840 Gal and 30-88 cm/s, respectively. The largest acceleration (822Gal) and seismic intensity (6.2) in the DCRC network was observed at No.9. At the other organizations, 1517 Gal was observed at K-NET 013, where boil sand and acceleration spikes probably due to soil liquefaction were observed. In Sendai, the 4/7 aftershock also caused severe damage, as did the mainshock. PGA and PGV of this aftershock range 167-767 Gal and 14-76 cm/s, respectively.

Fig. 3 shows the mainshock velocity waveforms in observation components near NS direction at all DCRC stations, with JMA E06, K-NET MYG013, and ground station of Izumi electric power building (IZU), Tohoku Electric Power Co. Velocity waveforms in Fig. 3 are calculated from acceleration records with low-cut frequency of 0.02Hz. Two major wave groups (hereafter Part A and Part B of the mainshock) can be commonly identified. There are gaps in waveforms at some QDR stations in Table 2. This gap is due to limitation of QDR that the record length of one file is up to 100s.

Fig. 4 compares pseudo velocity response spectra (5% damping) at stations locating east and west sides of Nagamachi-Rifu fault. The spectrum at No.27, locating near Sendai railway station, is commonly plotted in each side as a reference, because this station locates on the engineering bedrock as shown in Table 1. Spectra at west sides are equal to or relatively larger at short period (less than 1 second) than the No.27 spectrum, while the spectra at east sides are significantly larger than the No.27 spectrum, especially around 1 and 3 seconds. This is clearly due to the difference of subsurface structures described before.

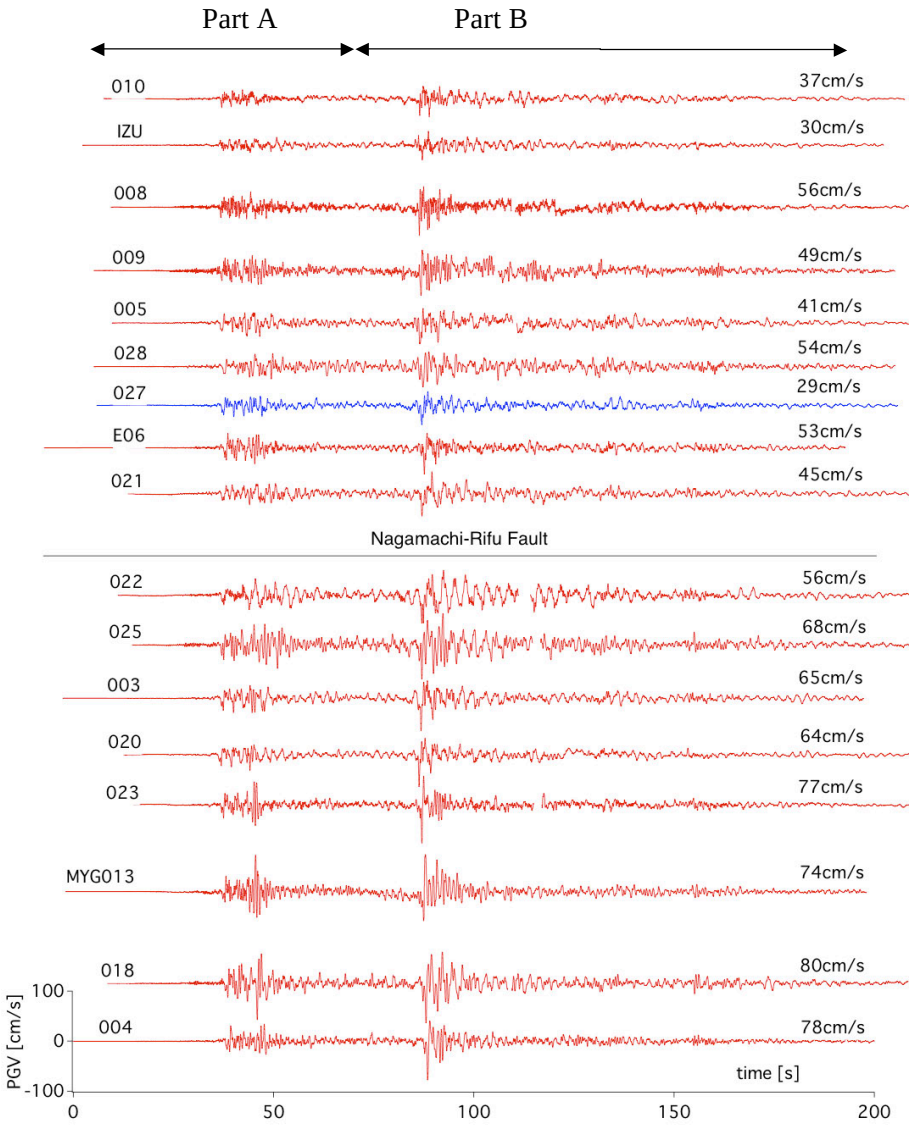

Fig. 3 Velocity waveforms of the DCRC records for the 2011 Tohoku earthquake

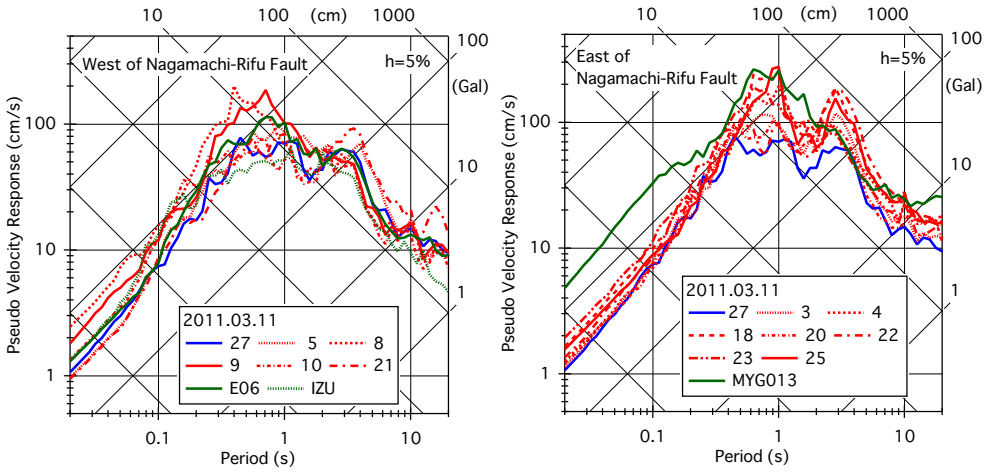

Fig. 4 Pseudo velocity response spectra of the DCRC records for the 2011 Tohoku earthquake

Table 2 List of earthquake records by DCRC strong-motion network, Tohoku University

Origin Time (JST)			2011/4/11			2011/4/7			2011/3/11			2011/3/9		
Area			Eastern Fukushima Pref.			Off Miyagi Pref.			2011 Tohoku Eq.			Far E Off Miyagi Pref.		
Mw, Depth			Mw 6.6, Depth 6km			Mw 7.1, Depth 66km			Mw 9.0, Depth 24km			Mw7.2, Depth 8km		
Type			Shallow Inland			IntraSlab			Subduction			Subduction		
No	Sensor	Station	PGA (cm/s^2)	PGV* (cm/s)	JMA Int.	PGA (cm/s^2)	PGV* (cm/s)	JMA Int.	PGA (cm/s^2)	PGV** (cm/s)	JMA Int.	PGA (cm/s^2)	PGV* (cm/s)	JMA Int.
2	ETNA	Rokugo Elementary School	54	5.5	3.9	311	42.1	5.7	Missing			Missing		
3	ETNA	Furujiro Elementary School	48	7.3	3.7	251	22.4	5.1	320	59.5	5.7	24	3.1	3.3
4	ETNA	Higashi Rokugo Elementary School	Removed			Removed			613	74.2	6.0	29	3.4	3.4
5	QDR	Daiichi Jr. High School	47	6.3	3.8	230	19.3	5.1	383	39.4	5.6	28	2.9	3.5
8	QDR	Shogen-Chuoh Elementary School	76	5.3	3.9	534	25.3	5.5	840	60.4	6.0	30	2.2	3.2
9	QDR	Matsumori Elementary School	Missing			767	75.5	6.2	822	85.7	6.4	46	4.2	3.7
10	QDR	Miyagi Prefecture Library 1F	Missing			279	18.0	5.0	407	62.7	5.6	20	2.4	3.2
12	QDR	Seiryo SecondarySchool 1F	30	5.4	3.7	Missing			Missing			19	3.5	3.3
14	QDR	Tsurugaya Elementary School 1F	48	4.3	3.5	432	30.6	5.7	Missing			20	1.9	3.1
16	QDR	Nakano Jr. High School 1F	81	7.8	4.3	Missing			Missing			40	3.2	3.6
18	QDR	Okino Elementary School 1F	71	6.9	4.1	360	31.8	5.6	512	77.6	6.2	37	3.5	3.5
20	QDR	Minami Koizumi Elementary School	34	6.6	3.6	220	25.7	5.3	381	63.0	5.6	19	2.4	3.1
21	QDR	Nishitaga Jr. High School	54	6.4	3.9	186	16.4	5.0	400	45.1	5.5	23	3.0	3.4
22	QDR	Tomizawa Jr. High School	53	8.8	3.9	232	21.1	5.2	416	54.6	5.7	29	3.2	3.4
23	QDR	East Water Supply Center	95	6.0	4.1	472	37.3	5.8	613	75.4	6.1	30	2.6	3.3
24	QDR	Ryutaku-Ji	Removed			Removed			Missing			Missing		
25	QDR	Nagamachi Minami Community Center	Missing			264	29.5	5.5	494	69.3	6.0	59	6.0	4.0
26	QDR	Aoba Ward Office	43	6.0	3.7	318	21.9	5.2	Missing			24	3.2	3.3
27	SSA-1	Sumitomo Seimei Bldg.	31	3.9	3.5	167	14.0	4.9	318	29.2	5.3	15	2.2	3.1

* cut-off period of 10s, ** cut-off period of 10s, ** 50s

SITE AMPLIFICATION FACTORS

Fig. 5 compares pseudo velocity response spectra in NS component from the 3/9 foreshock to the 4/11 aftershock at No.8 (northwestern side), No. 27 (near Sendai station), No.23 (Oroshi-machi, east side of the fault), No.25 (southeastern side) stations. It is found that the amplitudes of Part B are equal to or larger than that of Part A of the mainshock, and the short-period amplitude of the 4/7 aftershock is almost the same as that of Part A of the mainshock at some stations. At No.25, two predominant periods (around 3s and less than 1s) can be identified and the shorter predominant period clearly shows dependency on the amplitude level. This may due to the nonlinearity of the surface soil.

In Fig. 5, soil amplification factors from seismic bedrock to ground surface are also plotted. These amplification factors are calculated by equivalent linear analysis described in the later section with subsurface structure in Table 1. Long predominant period amplification, affected by deep underground structure from seismic bedrock, commonly appear around 2-3s at 4 stations. At periods shorter than 1s, the predominant period and amplification factors are strongly affected by shallow subsurface structure above engineering bedrock. Thus variations of the short-period amplifications at deep alluvial sites, No.23 and 25, are larger than those of the other two stations due to the nonlinear soil amplification.

Fig. 6 compares empirical (response spectral ratio of NS components) and theoretical amplification factors (1-D amplification shown in Fig. 5) at No.8, 23, 25 versus No.27. Although the empirical ratios are scattered, the period characteristics are similar to the theoretical ratios at periods shorter than 1s. At periods longer than 1s, almost no amplification is expected at No.25 by the 1-D theory, while about twice amplifications around 3s are calculated by the observation. This difference is probably due to the surface waves, as clearly shown in the later phases at southern area (No. 22 and 25) in Fig. 4

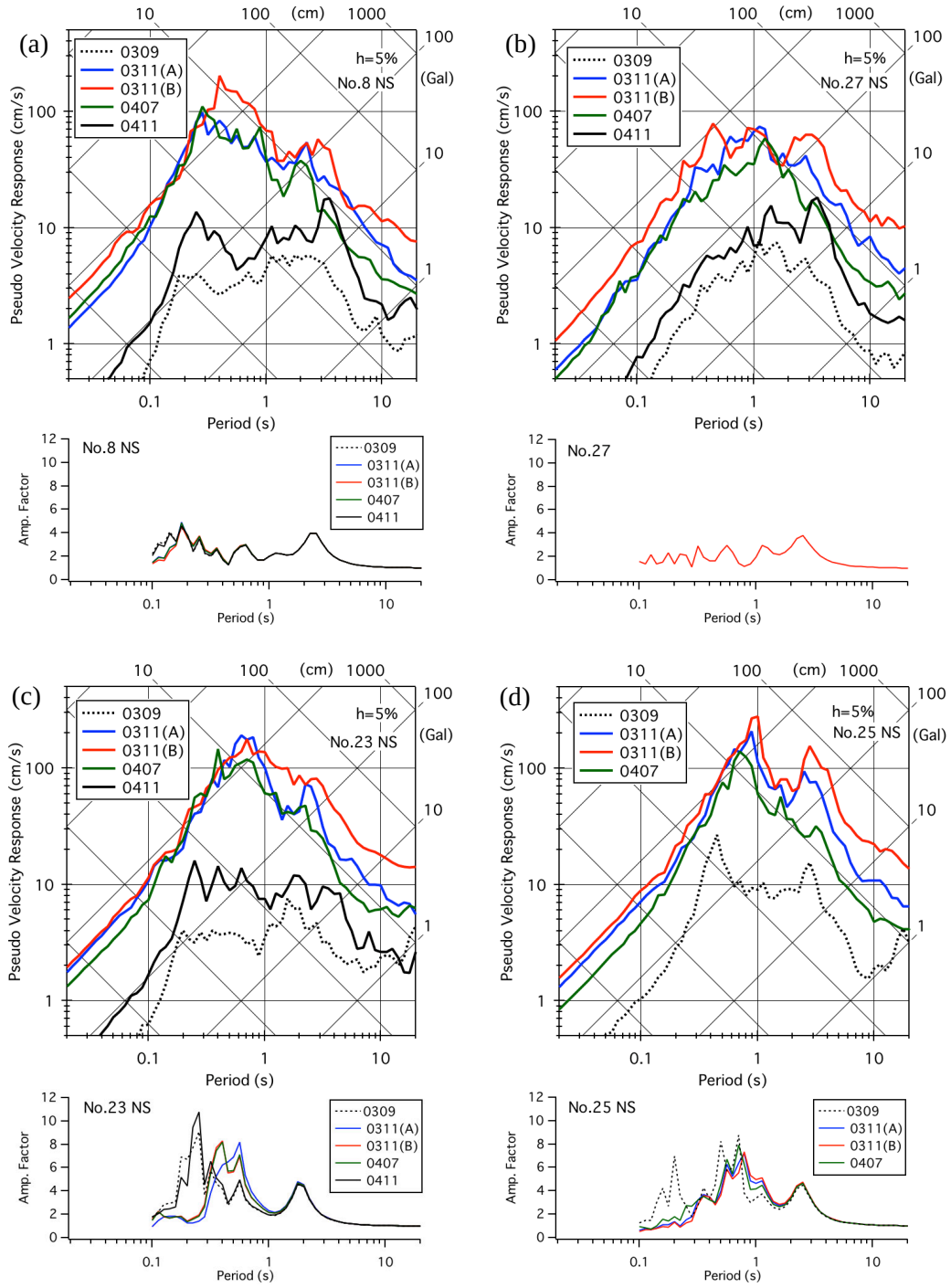

Fig. 5 Pseudo velocity response spectra and equivalent linear soil amplification factors of the DCRC records for the 2011 Tohoku earthquake sequence

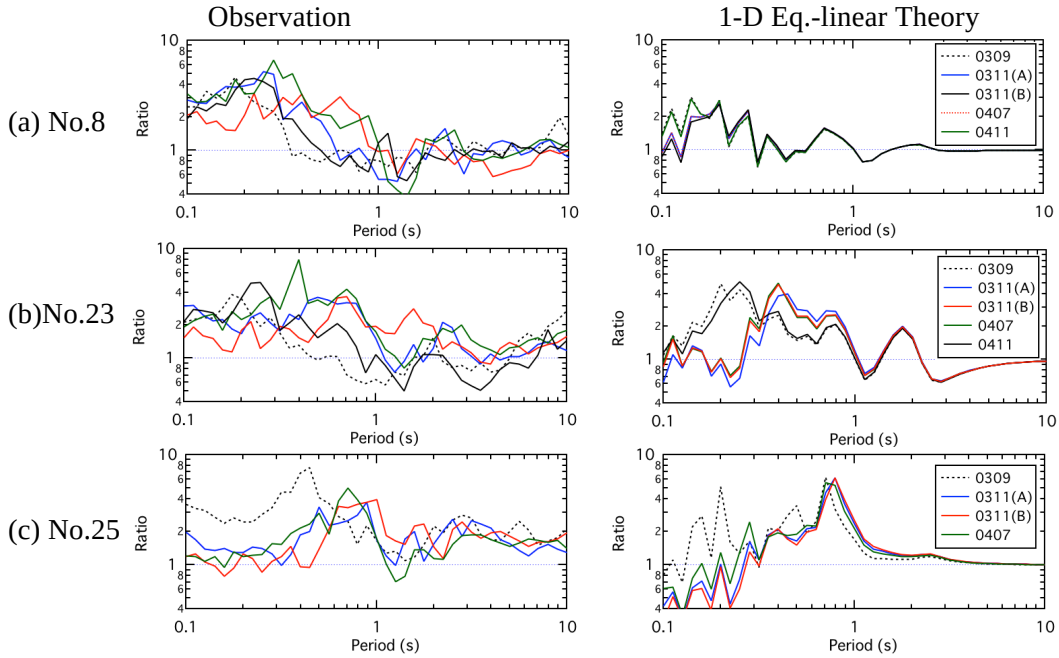

Fig. 6 Ratios of observed response spectra and theoretical amplification factors versus those of No.27 station

DISTRIBUTION OF RESPONSE SEPCTRA

Using the method of Ohno and Shibayama (2010), we estimate distribution of response spectra at ground surface in 250m-mesh over the city area of Sendai. Fig. 7 shows a flowchart of the method, which takes into account the effects of subsurface structure including nonlinear amplification of surface soil and spatial correlation of the spectra. The procedure is composed of 3 steps: 1) estimate response spectra at outcropped seismic bedrock at observation station location, by recursively applying equivalent linear spectral modal analysis of 1-D subsurface structure (linear analysis for the part deeper than engineering bedrock), 2) estimate spatial correlation of outcropped spectra and interpolate in 250m-mesh by ordinary kriging method, 3) estimate ground surface spectrum in each mesh by equivalent linear spectral modal analysis.

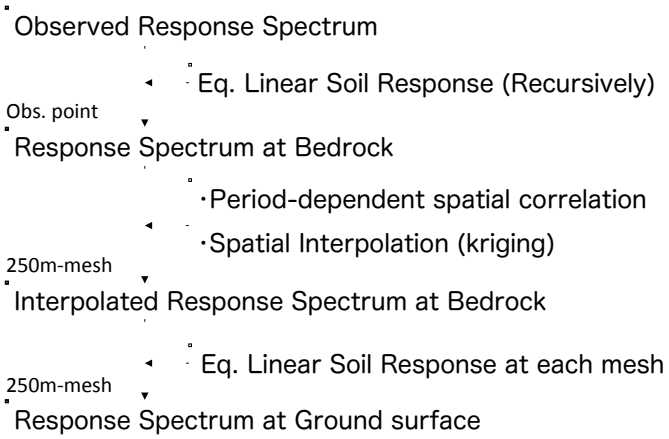

Fig.7 Flowchart of estimating distribution of response spectra in Sendai (Ohno and Shibayama, 2010)

We used the subsurface structure model (including nonlinear soil properties of soil) in Sendai City (2002) and used the records of DCRC, JMA, NIED, PARI, BRI, Tohoku Electric Power Company. Fig. 8 and Fig. 9 show the estimation results at periods of 0.2, 1, and 3.2s for parts A and B of the mainshock, and for the 4/7 and 4/11 aftershocks. The following tendencies are found:

1) Strong-shaking areas are different by period. At 0.2s, amplitude at the northwestern area is larger than the other area. This is due to the shallow soil over engineering bedrock. An exception is the 4/11 shallow inland aftershock, probably due to the lack of short-period incident waves by strong attenuation in propagating the shallow crust.
   At 1.0s, amplitudes at the eastern side of Nagamachi-Rifu fault are larger, due to the surface soil amplification.
   At 3.2s, amplitudes at the southern area are larger, due to the deep underground structure including existence of surface waves as discussed before. The 4/11 aftershock again shows a different distribution. In this earthquake, large amplitude area expands from southern side to northwestern side. The similar distribution was found for the 6/14/2008 Iwate-Miyagi-Nairiku shallow inland earthquake (Ohno and Shibayama, 2010).
2) The amplitudes of Part A are larger than those of Part B during the mainshock.
3) Amplitudes at NS direction are larger than those at EW direction during the mainshock (Parts A and B), while EW direction is predominant at the 4/7 aftershock. At the 4/11 aftershock, NS direction is significantly predominant at long periods.

CONCLUSIONS

Site amplifications and distribution of strong-motion spectra in Sendai are estimated for the 2011 Tohoku earthquake sequences by using the DCRC strong-motion network records and subsurface structure models in Sendai.

Short-period (less than 1 second) amplifications are observed in the northern area, while not only short but also long-period (around 3s) amplifications were observed in the southern area. Also, significant amplitude-dependencies of predominant periods were shown at some alluvial sites. This short period amplifications are mainly due to the shallower part above engineering bedrock. The long-period amplifications are partly explained by 1-D response of subsurface structures above seismic bedrock, while surface wave contribution cannot be ignored at some sites locating southern part of Sendai.

ACKNOWLEDGMENTS

Strong motion records from National Research Institute for Earth Science and Disaster Prevention (NIED), Port and Airport Research Institute (PARI), Japan Meteorological Agency (JMA), Building Research Institute (BRI), and Tohoku Electric Power Company are used.

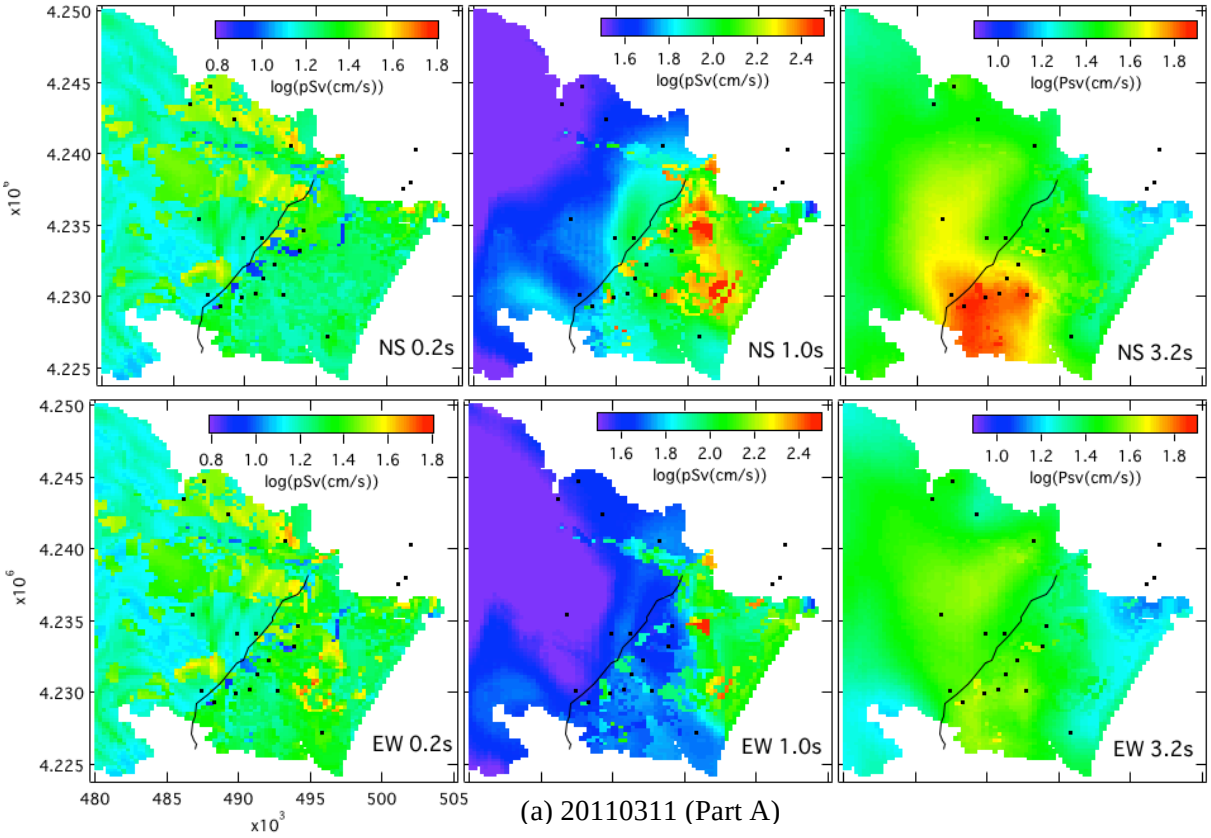

(a) 20110311 (Part A)

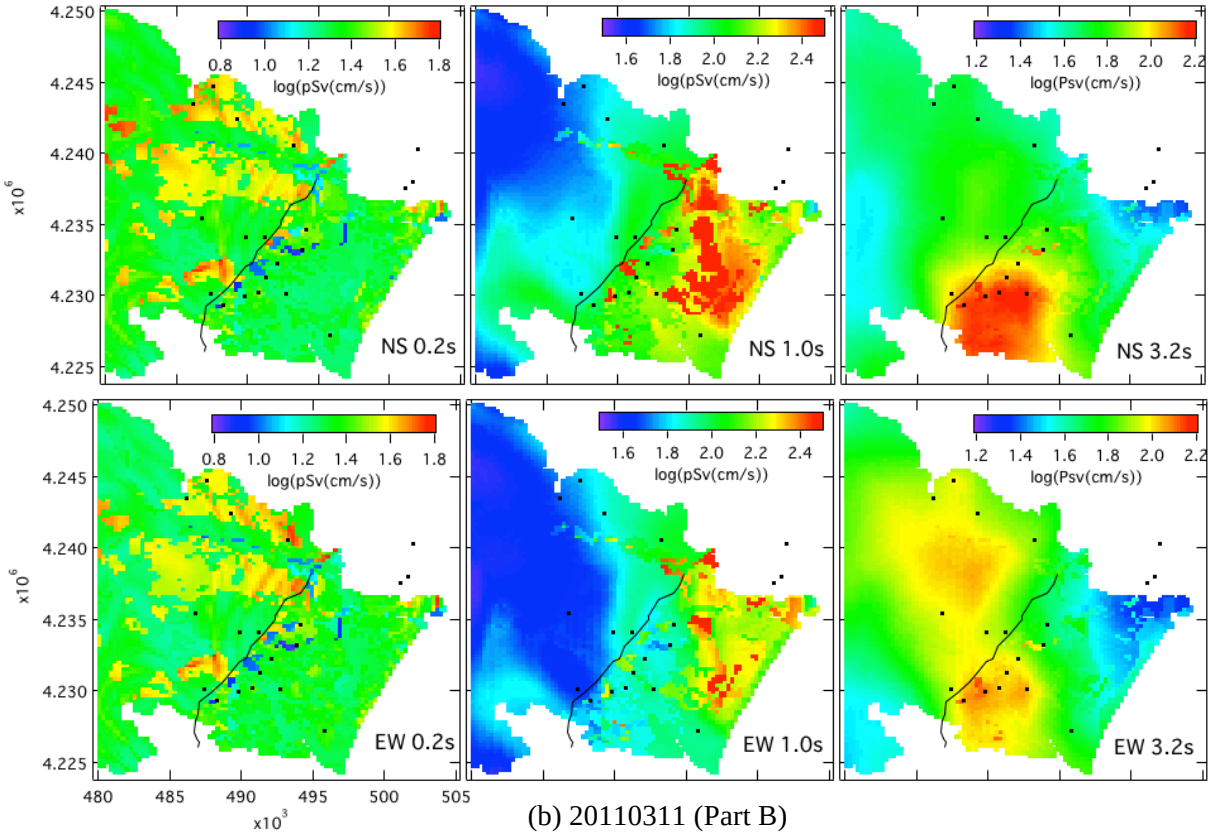

(b) 20110311 (Part B)

Fig. 8 Estimated distribution of response spectra at ground surface for the 2011 Tohoku earthquake

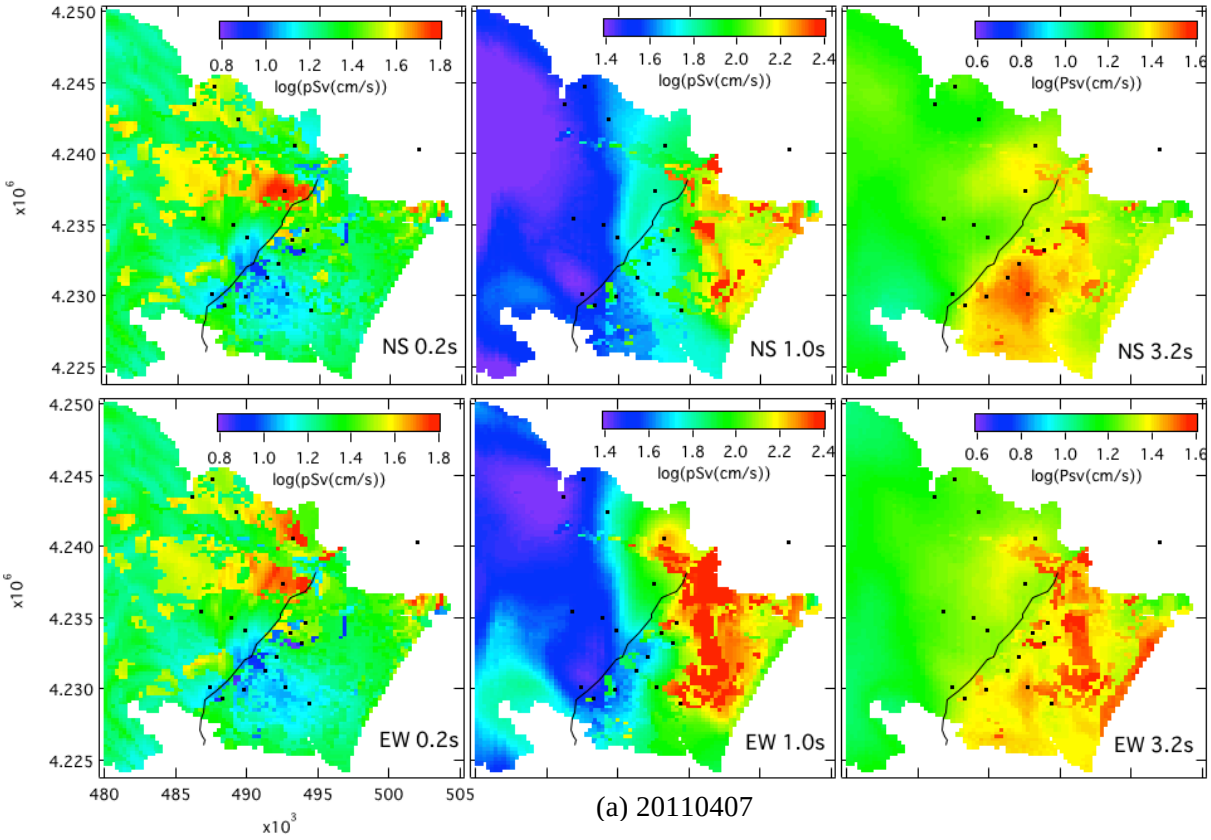

(a) 20110407

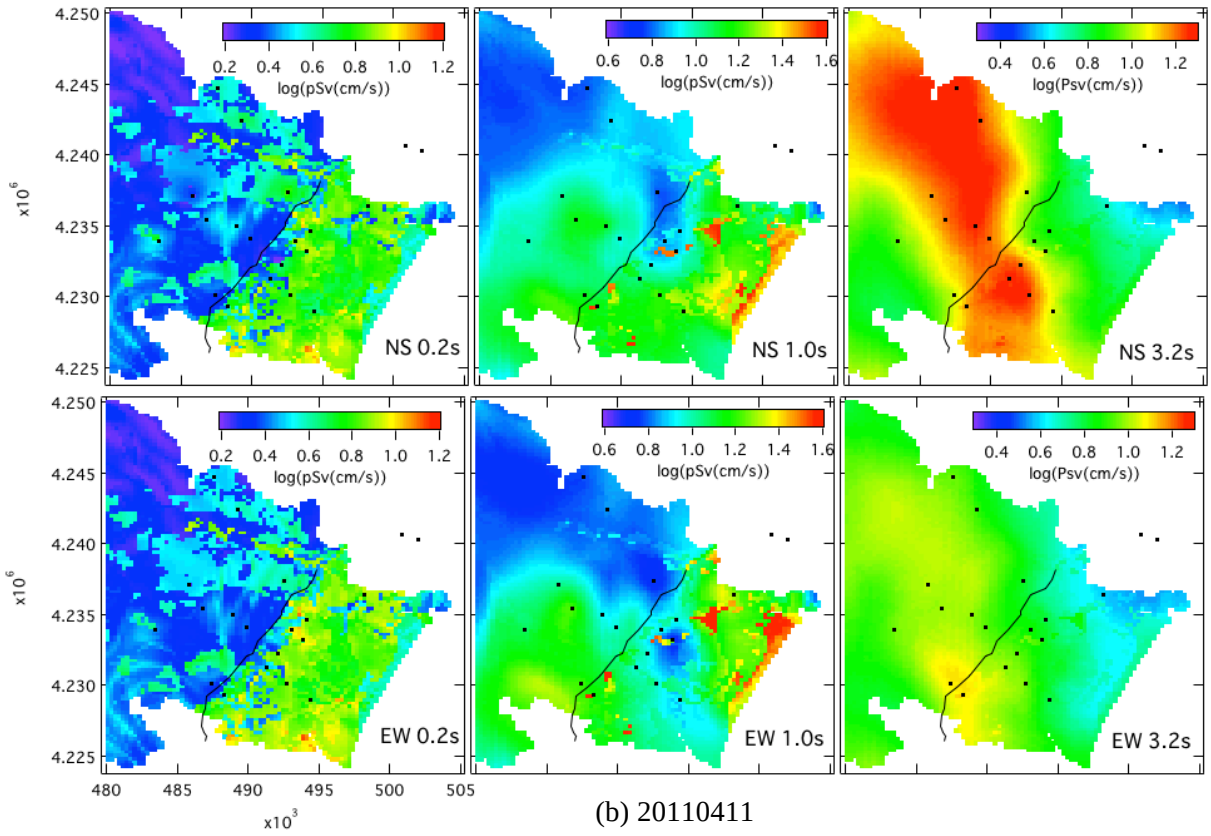

(b) 20110411

Fig. 9 Estimated distribution of response spectra for the aftershocks of the 2011 Tohoku earthquake

REFERENCES

Building Research Institute and Japan Association for Building Research Promotion (1999). "*Sendai high-density strong-motion array comprehensive report*". (in Japanese)

Kamiyama, M., Shoji, Y. , Matsukawa, T., Asada, A., and Nakai, N. (2001). "An On-Line Array Observation System of Earthquake Motions: The Deployment and Records", *Journal of Structural Mechanics and Earthquake Engineering*, Vol. 698, 283-298. (in Japanese with English Abstract)

Kamiyama, M. (2011). http://www.st.hirosaki-u.ac.jp/~kataoka/Tohoku_EQ/Kamiyama__SmallTitan_01.pdf. (in Japanese)

Ohno, S., Motosaka, M., Sato, T., and Yamamoto, Y. (2004). "Strong-motion Observation Network for Seismic Capacity Evaluation of Buildings in Sendai, Japan", *Summaries of Technical Papers of Annual Meeting, Architectural Institute of Japan*, Structures II, 1075-1076. (in Japanese)

Ohno, S. and Shibayama, A. (2010). "Estimation of spatial distribution of response spectra considering soil amplification and spatial correlation of ground motions", *Proc. 13th Japan Earthquake Engineering Symposium*, GO1-Thu-PM-10. (in Japanese with English Abstract)

Satoh, T., Kawase, H. and Sato, T. (1994). Engineering bedrock waves obtained through the identification analysis based on borehole records and their statistical envelope characteristics, *Journal of Structural and Construction Engineering*, No. 461, 19-28. (in Japanese with English Abstract)

Sendai City (2002). "Heisei 14 Fiscal Year Earthquake Damage Estimation Report". (in Japanese)

Watanabe, T. and Motosaka, M (2002). "Estimation of Deep Underground Structure in Sendai Area based on Microtremor Observations and Strong-motion Prediction", *Proc. AIJ Tohoku Chapter Architectural Research Meeting*, No.65, 133-136. (in Japanese)